

Dynamics of quantum entanglement

Karol Życzkowski,^{1,2,*} Paweł Horodecki,^{3,†} Michał Horodecki,^{4,‡} and Ryszard Horodecki^{4,§}

¹Centrum Fizyki Teoretycznej PAN, Al. Lotników 32/46, 02-668 Warszawa, Poland

²Instytut Fizyki im. Smoluchowskiego, Uniwersytet Jagielloński, ul. W. Reymonta 4, 30-059 Kraków, Poland

³Wydział Fizyki Technicznej i Matematyki Stosowanej, Politechnika Gdańska, ul. G. Narutowicza 11/12, 80-952 Gdańsk, Poland

⁴Instytut Fizyki Teoretycznej i Astrofizyki, Uniwersytet Gdański, ul. Wita Stwosza 57, 80-952 Gdańsk, Poland

(Received 20 September 2000; published 10 December 2001)

A model of discrete dynamics of entanglement of a bipartite quantum state is considered. It involves a global unitary dynamics of the system and periodic actions of local bistochastic or decaying channel. For initially pure states the decay of entanglement is accompanied by an increase of von Neumann entropy of the system. We observe and discuss revivals of entanglement due to unitary interaction of subsystems. For some mixed states having different marginal entropies of the subsystems we find an asymmetry in speed of entanglement decay. The entanglement of these states decreases faster, if the depolarizing channel acts on the “classical” subsystem, characterized by smaller marginal entropy.

DOI: 10.1103/PhysRevA.65.012101

PACS number(s): 03.65.Ta, 03.67.-a

I. INTRODUCTION

Quantum entanglement is one of the most subtle and intriguing phenomena in nature [1,2]. Its potential usefulness has been demonstrated in various applications such as quantum teleportation, quantum cryptography, and quantum dense coding. On the other hand, quantum entanglement is a fragile feature, which can be destroyed by interaction with the environment. This effect due to *decoherence* [3], is the main obstacle for practical implementation of quantum computing. A model allowing to study the dynamics of entanglement in presence of interaction with the environment has been recently analyzed by Yi and Sun [4].

In this paper we investigate destruction of the entanglement in a proposed model of discrete dynamics. We consider a simple bipartite system consisting of two spin-1/2 particles. Only one of them is subjected to periodic actions of a quantum channel, which represents the interaction with environment. As the initial states we choose random states taken from the ensemble of pure separable states and from the ensemble of maximally entangled pure states. We also investigate the time evolution of mixed states having some special property. The corresponding system is composed of two subsystems exhibiting different properties with respect to some entropy inequality that is satisfied by all classical systems. One of the subsystems satisfies the inequality and may be considered “classical,” while the other, “quantum” subsystem, violates the inequality. We investigate an asymmetry in the process of destruction of entanglement with respect to the subsystem interacting with the environment. We demonstrate a possible presence of revivals of entanglement caused by the global unitary evolution entangling the subsystems between consecutive actions of the environment.

The paper is organized as follows. In Sec. II we describe

a simple model of discrete time evolution. In Sec. III we derive bounds on the entropy increase under the action of the environment. Then in Sec. IV we analyze the decrease of entanglement versus increase of the degree of mixing of the initially pure states. The asymmetry in the entanglement decay depending on the subsystem subjected to influence of environment is described in Sec. V. In Sec. VI we consider the entanglement revivals. The results of the paper are discussed in Sec. VII.

II. MODELS OF TIME EVOLUTION

In this paper we consider the bipartite state subjected sequential interactions with environment. They are modeled by quantum channels, defined as completely positive linear maps, preserving the trace of the state [5].

Let σ be a density operator acting on a finite-dimensional Hilbert space \mathcal{H} . The most general form of the quantum channel is the following transformation $\sigma \rightarrow \sigma'$:

$$\sigma' \equiv \Lambda(\sigma) = \sum_{i=1}^K V_i \sigma V_i^\dagger, \quad \text{where} \quad \sum_{i=1}^K V_i^\dagger V_i = \mathbb{I}. \quad (1)$$

If in addition $\sum_{i=1}^K V_i V_i^\dagger = \mathbb{I}$ holds then the channel is called *bistochastic*.

Bistochastic channels can be alternatively defined as channels that do not decrease von Neumann entropy of quantum states.

A particular example of the bistochastic channel is given by *random external fields* [6]. They can be written as

$$\sigma' \equiv \Lambda_R(\sigma) = \sum_{i=1}^K p_i A_i \sigma A_i^\dagger, \quad (2)$$

where A_i , $i=1,2,\dots,K$ are *unitary* operators and the vector of probabilities $\vec{p} = [p_1, \dots, p_K]$ is normalized

$$\sum_{i=1}^K p_i = 1, \quad p_i \geq 0. \quad (3)$$

*Electronic address: karol@cft.edu.pl

†Electronic address: pawel@mifgate.pg.gda.pl

‡Electronic address: michalh@iftia.univ.gda.pl

§Electronic address: fizrh@univ.gda.pl

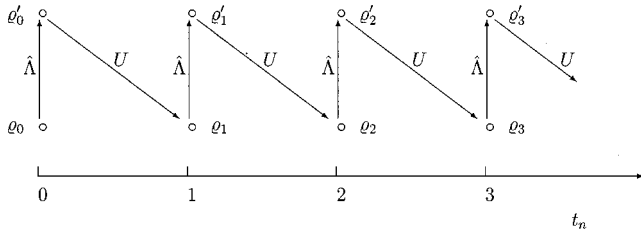


FIG. 1. Discrete model of periodic dynamics (5), (cf. Figs. 8.1 and 8.2 of Ref. [10]). Interaction with the environment $\hat{\Lambda}$ transforms the state q_n into q'_n and then the unitary transformation U maps it into q_{n+1} .

Such random systems can be described in the formalism of *quantum iterated function systems* [7]. The so-called Kraus form (1) can be reproduced setting $V_i = \sqrt{p_i} A_i$. It is worth noting that in the case of the most elementary quantum system described on the Hilbert space $\mathcal{H} = \mathbb{C}^2$ the channel is bistochastic *if and only if* it is a random external field (2) (see [8]). Note that an unitary evolution of the system can be considered as the simplest case of the bistochastic quantum channel with $K = 1$.

There exist, however, many quantum channels that are not bistochastic. We shall consider the following *decaying channel*, sometimes called [9] the *amplitude damping channel*

$$\sigma' \equiv \Lambda_D(\sigma) = M_1 \sigma M_1 + M_2 \sigma M_2, \quad (4)$$

where the matrices

$$M_1 = \begin{bmatrix} 1 & 0 \\ 0 & \sqrt{p} \end{bmatrix}$$

and

$$M_2 = \begin{bmatrix} 0 & \sqrt{1-p} \\ 0 & 0 \end{bmatrix}$$

are written in the standard basis.

Let ϱ denote a mixed state of a $2 \otimes 2$ system i.e., the density operator defined on the Hilbert space $\mathcal{H} = \mathcal{H}_A \otimes \mathcal{H}_B = \mathbb{C}^2 \otimes \mathbb{C}^2$. The system consists of two subsystems A and B that can represent spin-1/2 particles or two-level atoms. In our model the unitary dynamics is interrupted by periodic actions of the environment as shown schematically in Fig. 1.

Discrete time evolution of the state ϱ reads in our model

$$\varrho(n+1) = U \varrho'(n) U^\dagger = U \{ \hat{\Lambda}[\varrho(n)] \} U^\dagger, \quad (5)$$

where $\hat{\Lambda} = I \otimes \Lambda$ and the channel Λ is either bistochastic (2) or decaying (4). Here $U = e^{i\alpha \tilde{H}}$ represents a unitary transformation that involves an interaction between the two subsystems A and B described by the Hamiltonian \tilde{H} . We use the dimensionless units and α stands for a coupling parameter. Subsequently we shall consider the cases with \tilde{H} equal either to $\sigma_x \otimes \sigma_y \equiv H$ or to $\tilde{H} = \sigma_y \otimes \sigma_x \equiv H'$.

In general we shall use four types of dynamics defined by four different operators Λ 's in the formula (5). Three of them

will be random external fields Λ_R (2), all defined by the same set of $K = 4$ unitary operators: $A_1 = I$, $A_2 = \sigma_1$, $A_3 = \sigma_2$, $A_4 = \sigma_3$ (where σ_i denote Pauli matrices), but with different vectors of probability (3):

$$\vec{p}^{(1)} = (1 - \epsilon, 0, 0, \epsilon),$$

$$\vec{p}^{(2)} = \left(1 - \epsilon, 0, \frac{\epsilon}{2}, \frac{\epsilon}{2} \right),$$

$$\vec{p}^{(3)} = \left(1 - \epsilon, \frac{\epsilon}{3}, \frac{\epsilon}{3}, \frac{\epsilon}{3} \right), \quad 0 \leq \epsilon \leq 1. \quad (6)$$

Each dynamics depends on two continuous parameters: α contained in $U = e^{i\alpha \tilde{H}}$ governing the unitary dynamics and ϵ , included in the vector of probabilities, and describing the strength of the coupling with the environment. Additional discrete index j labels the different vectors of probability $\vec{p}^{(j)}$. For these three models of dynamics we shall use the compact notation $\Theta_{\alpha, \epsilon}^j$. The fourth dynamics denoted by $\Theta_{\alpha, p}$ is defined by putting in formula (5) the decaying channel (4). Dynamics involving the operation U with “reflected” (i.e., obtained from H by permutating subsystems) Hamiltonian $H' = \sigma_y \otimes \sigma_x$ will be denoted by the same symbols with only one change: $\Theta \rightarrow \tilde{\Theta}$.

Remark. If α is equal to zero, then the unitary operation U in Eq. (5) is reduced to identity transformation. In particular, it can be seen that the dynamics $\Theta_{0, \epsilon}^3$ corresponds to periodic action of *depolarizing channel* [11].

Now the essence of our study is the following: we consider composite quantum systems subjected to the local interaction with the environment, which acts on one subsystem only. We investigate how the decay of the entanglement in the system depends on the initial state and the type of the dynamics. In particular we analyze to which extent the decrease of the mean entanglement is reflected by the evolution of von Neumann entropy of the system.

III. BOUNDS ON ENTROPY INCREASE UNDER LOCAL CHANNEL

We start establishing bounds for the increase of von Neumann entropy.

Proposition. Under a local action of the quantum channel $\varrho_{AB} \rightarrow (I \otimes \Lambda) \varrho_{AB}$, the increase of the von Neumann entropy ΔS for a bipartite $n \otimes m$ state is bounded by

$$\Delta S \equiv S(\varrho_{AB}^{\text{out}}) - S(\varrho_{AB}^{\text{in}}) \leq S(\varrho_A^{\text{in}}) - S(\varrho_{AB}^{\text{in}}) + \ln m, \quad (7)$$

where $S(\varrho_A)$ denotes the entropy of the subsystem A . In particular, if the system is separable then $\Delta S \leq \ln m$.

Proof. By definition the local channel is trace preserving, hence it does not change the density matrix of the first subsystem. Thus $\varrho_A^{\text{out}} = \varrho_A^{\text{in}}$ and the same holds for the corresponding entropies. Then from subadditivity of the entropy we have

$$\begin{aligned}
 S(\varrho_{AB}^{\text{out}}) &\leq S(\varrho_A^{\text{out}}) + S(\varrho_B^{\text{out}}) \\
 &= S(\varrho_A^{\text{in}}) + S(\varrho_B^{\text{out}}) \leq S(\varrho_A^{\text{in}}) + S_{\text{max}}^B \\
 &\equiv S(\varrho_A^{\text{in}}) + \ln m. \tag{8}
 \end{aligned}$$

We get the first inequality in the Proposition by subtracting $S(\varrho_{AB}^{\text{in}})$ from both sides of the above inequality. For separable states one always has $S(\varrho_{AB}^{\text{in}}) - S(\varrho_A^{\text{in}}) \geq 0$ [12] that simplifies Eq. (7) to $\Delta S \leq \ln m$ as expected.

Note that a sequence of quantum channels acting locally forms a quantum channel acting locally too. So the proposition works also for the dynamics $\Theta_{0,\epsilon}^i$ and $\Theta_{0,p}$. Moreover, from Eq. (7) we see that the entropy of initially pure separable state ϱ_{AB}^{in} cannot exceed $\ln m$.

IV. ENTANGLEMENT VERSUS DEGREE OF MIXING

In this section we study the time evolution of entanglement and compare it with the time evolution of von Neumann entropy. To characterize the degree of entanglement we use the *entanglement of formation* introduced by Bennett *et al.* [11]. For any $2 \otimes 2$ mixed state this quantity may be computed analytically as shown by Hill and Wootters [13]. In this case the entanglement of formation E (or shorter, the entanglement) varies from zero (separable states) to $\ln 2$ (maximally entangled states), so in the figures we used the rescaled variable $E/\ln 2$.

Our results were obtained by averaging over ensembles of random initial states. They were generated according to natural measures on (i) six-dimensional manifold of all pure states for $2 \otimes 2$ problem, (ii) three-dimensional manifold of maximally entangled pure states, and (iii) four-dimensional manifold of separable pure states.

Numerical experiments have shown that the samples of 100 initial states, generated randomly as described in the Appendix, were sufficient to receive reliable results.

A. Bistochastic channels

As shown in Refs. [14,15] the mean entanglement of mixed states decreases monotonically with increasing degree of mixing. Due to interaction with the environment the initially pure states become mixed: their von Neumann entropy, $S(\varrho) = -\text{Tr}(\varrho \ln \varrho)$, grows in time. Thus it is natural to expect a corresponding monotonous decay of the mean entanglement. This indeed takes place, as shown in Fig. 2, in absence of the unitary dynamics, ($\alpha=0$). Initial states were taken randomly from the entire space of pure states, so in accordance with [15], the initial mean entanglement is close to $(\ln 2)/2$. The parallel processes of decay of the entanglement and increase of the entropy are accelerated, if the parameter ϵ describing the interaction with environment increases.

For initially maximally entangled pure states [case (ii)] a similar dependence is represented by circles in Fig. 3. Here $\langle E(0) \rangle = \ln 2$. The picture changes when unitary evolution is involved. The latter leads to oscillations of entanglement of formation, reflected in the time evolution of entropy. The

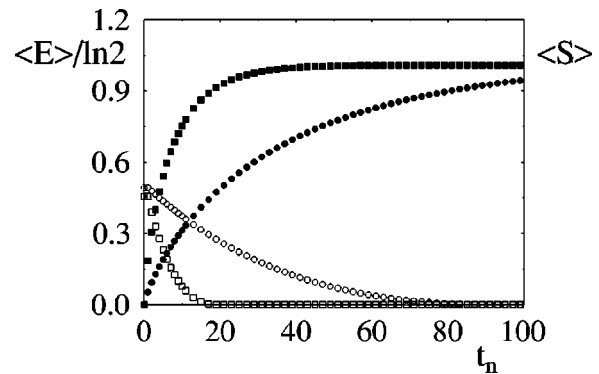


FIG. 2. Dynamics of quantum entanglement for system $\Theta_{0,\epsilon}^2$. Mean entanglement of formation $\langle E \rangle$ (open symbols) and von Neumann entropy $\langle S \rangle$ (closed symbols) averaged over a sample of 100 random pure states shown as functions of discrete time t_n . No unitary evolution is present, ($\alpha=0$). Parameter ϵ , controlling the interaction with environment is set to 0.01 (\circ) or 0.05 (\square).

frequency of oscillations is proportional to α . The larger this parameter, the faster the unitary evolution U rotates the states ϱ from and into the convex set of separable states. In the case of entropy, oscillations are only due to changes of the second derivative, i.e., entropy is still monotonically decreasing. This is not the case for entanglement E , which can also be seen in Fig. 4 for several individual initial states (without averaging). For short times the curve for $\alpha=0$ (no unitary evolution) seems to constitute an envelope for all other curves.

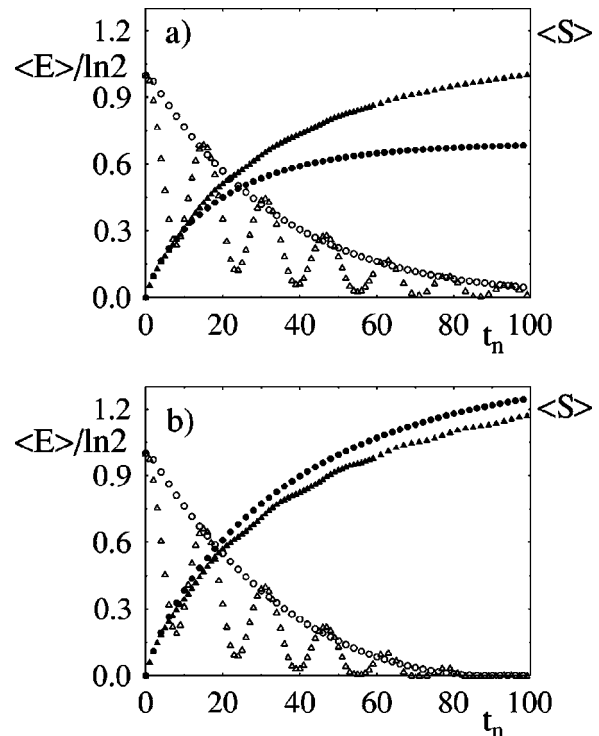


FIG. 3. As in Fig. 2 for a sample of 100 maximally entangled states [$E(0) = \ln(2)$] with $\epsilon=0.01$; $\alpha=0.0$ (\circ) and $\alpha=0.1$ (\triangle) for channels described by (a) $\vec{p}^{(1)}$ and (b) $\vec{p}^{(2)}$. Observe how the influence of the unitary dynamics depends on the kind of the channel.

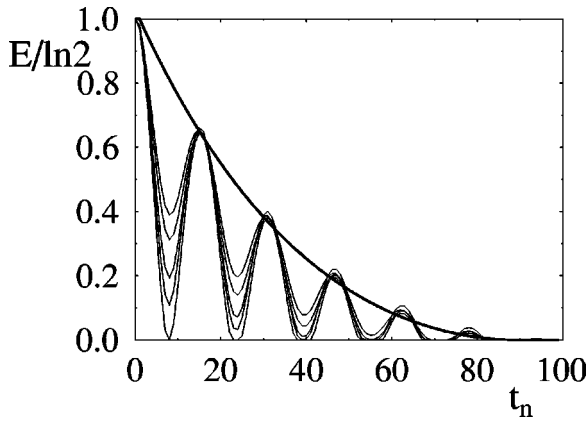


FIG. 4. Dependence of entanglement of formation on time for several randomly chosen maximally entangled pure states. The unitary dynamics $U = \exp(i\alpha\bar{H})$ is governed by the parameter α . Here $\epsilon = 0.01$ in $\bar{p}^{(2)}$, and $\alpha = 0.1$ (narrow lines). Reference bold line represents the case of no unitary dynamics ($\alpha = 0$), for which the dynamics of entanglement does not depend on the initial state.

It is worth emphasizing a significant difference between $\Theta_{\alpha,\epsilon}^1$ [Fig. 3(a)] and $\Theta_{\alpha,\epsilon}^2$ [Fig. 3(b)]. In the former case the presence of unitary evolution can accelerate the process of entropy increase. In the latter, on the contrary, switching on unitary evolution results in slower increase of the mean entropy. The iteration of the channel $\Theta_{\alpha,\epsilon}^1$ preserves both the number and the position of the nonzero component in \bar{p} . It is not the case for $\Theta_{\alpha,\epsilon}^2$, for which two Pauli matrices generate

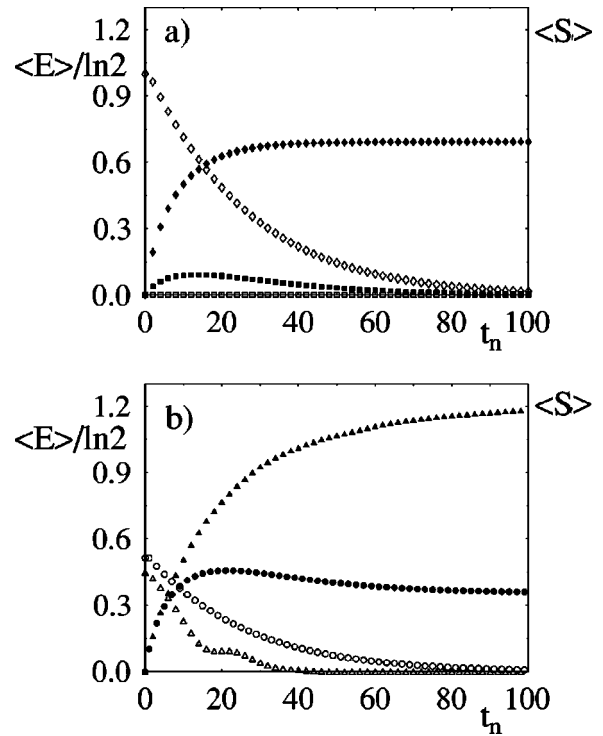


FIG. 6. As in Fig. 2 for samples of 100 pure states subjected to the Kraus channel (4) with $p = 0.05$ and $\alpha = 0.0$. Initial states drawn randomly from the ensembles of (a) (\square), separable pure states; (a) (\diamond), maximally entangled pure states, and (b) (\circ), ensemble of all pure states. Case (i) with unitary evolution, $\alpha = 0.1$, is denoted by (\triangle) in panel (b).

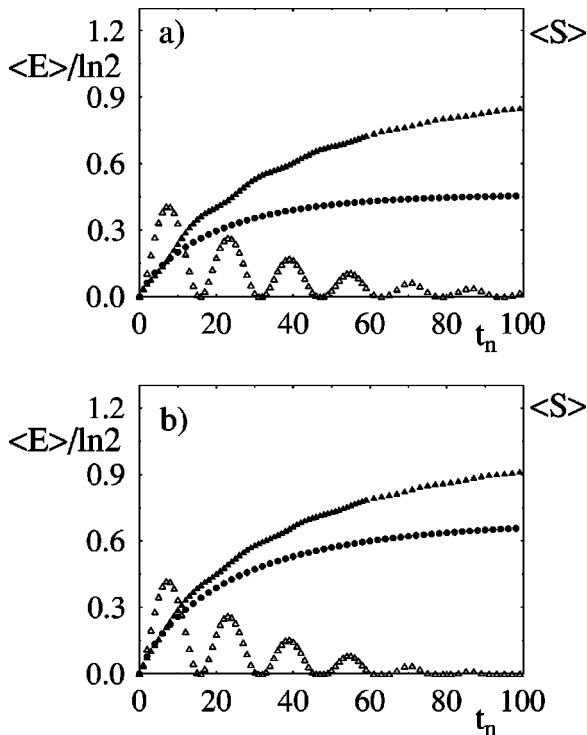


FIG. 5. As in Fig. 3 for a sample of 100 initially separable pure states [$E(0) = 0$]. In absence of unitary dynamics, ($\alpha = 0$), the entanglement equals zero.

the entire algebra of unitary matrices A_i involved.

Consider now the case (iii), of initially separable states, presented in Fig. 5. The presence of the unitary evolution may increase the mean entanglement, initially equal to zero. However, there is one difference more; for *both* dynamics $\Theta_{\alpha,\epsilon}^1$ [Fig. 5(a)] and $\Theta_{\alpha,\epsilon}^2$ [Fig. 5(b)] presence of the unitary dynamics accelerates the process of increase of entropy. In absence of the unitary dynamics ($\alpha = 0$) the entropy does not exceed the value $\ln 2$ in accordance to our proposition proved in Sec. III.

The obtained results show that the oscillations of the mean entanglement E are anticorrelated with the oscillations of the entropy S . It was also checked that if α is kept constant, but is the Hamiltonian is chosen randomly then the oscillations of entanglement are smeared out. It means that effects of quantum coherence are destroyed and the destruction of entanglement occurs faster.

B. Decaying channel

Figure 6 presents results obtained for the amplitude damping channel (4). In the absence of the unitary evolution ($\alpha = 0$) the mean entropy $\langle S \rangle$, averaged over the entire manifold of pure states [case (i)], does not tend monotonically to its maximal value. At $t_n \sim 20$ the entropy reaches its maximum and then decreases to its limiting value about 0.3 [see

full circles in Fig. 6(b)]. This is due to the fact that for the *decaying* channel the entropy of the system may decrease.

Numerical data received by averaging over the set of maximally mixed states [case (ii), diamonds] and the set of separable pure states [case (iii), squares] are shown in Fig. 6(a). Observe that the steady-state limiting values of the von Neumann entropy $\langle S \rangle$ represents the initial average entanglement $\langle E \rangle$. Indeed, in absence of the unitary evolution the perturbed subsystem is eventually dumped to the ground state. So finally the state of the system is a product of the ground state of the affected subsystem and the reduced density matrix of the unperturbed subsystem. Thus, after the averaging procedure, one gets the averaged von Neumann entropy of the subsystem not subjected to action of the channel.

A random choice of initially pure states of the composite system induces a certain measure in the space of the reduced density matrices [16]. As proved recently by Hall [17] the natural rotationally invariant measure on the space of $N=4$ pure states induces a uniform measure in the *Bloch ball* representing the density matrices for $N=2$. Denoting the spectrum of reduced matrices by $\{1/2-r, 1/2+r\}$ we may write more formally, $P(r) = 24r^2$ for $r \in [0, 1/2]$. The von Neumann entropy, averaged over this measure equals $1/3$ [17], in agreement with the numerical data presented in Fig. 6.

For nonzero values of α we observe the oscillations of the mean entanglement, caused by the unitary evolution. It is interesting, however, that the presence of unitary evolution allows the final entropy to be maximal [see full triangles in Fig. 6(b)] It means that the presence of the decay channel is *completely masked* by the unitary interaction between the two subsystems.

V. ASYMMETRY OF ENTANGLEMENT DECAY

We shall consider here dynamics of mixed states having an intriguing property. Namely, we choose a quantum bipartite system, which *violates some entropy inequality only with respect to one of both subsystems*. Let us recall first that the information gain resulting from the measurement of any of the subsystems of a quantum state with classical correlations is not greater than the gain obtained from measurement per-

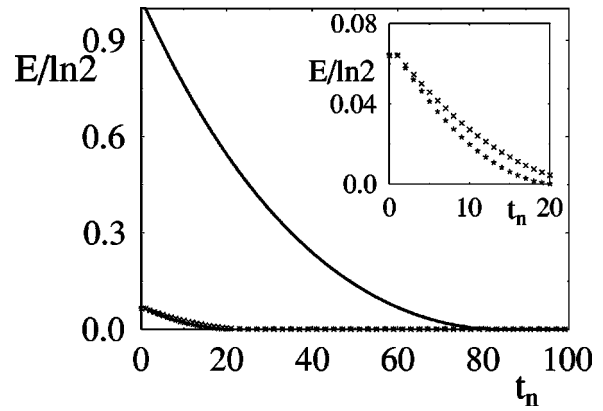


FIG. 7. Comparison of the dependence of the entanglement of formation for the state $\varrho^{(1)}$ with $a^2=3/4$; $q=3/5$ (\star) and $\varrho^{(2)}$ (\times). The bistochastic channel \bar{p}_3 with $\epsilon=0.01$ interacts with the “classical” subsystem B in the former case, and with the “quantum” subsystem A in the latter case. Solid line represents the behavior of a maximally entangled state ρ_{\max} . Magnification of the initial dependence provided in the inset reveals the asymmetry of the entanglement decay.

formed on the entire system. This classical feature is characteristic of quantum separable states. They do satisfy the following two inequalities concerning von Neumann entropy [12,18]:

$$S(\varrho_{AB}) \geq S(\varrho_A) \tag{9}$$

and

$$S(\varrho_{AB}) \geq S(\varrho_B), \tag{10}$$

where ϱ_A and ϱ_B denote the reduced density matrices, e.g., $\varrho_A \equiv \text{Tr}_B(\varrho_{AB})$. Now we shall focus on the following family of states introduced in Ref. [19]. They can be written as

$$\varrho^{(1)} := q|\Psi_1\rangle\langle\Psi_1| + (1-q)|\Psi_2\rangle\langle\Psi_2|, \quad 0 < q < 1,$$

with normalized pure state vectors $|\Psi_1\rangle = a|00\rangle + \sqrt{1-a^2}|11\rangle$ and $|\Psi_2\rangle = a|10\rangle + \sqrt{1-a^2}|01\rangle$ with $0 < a < 1$. In the standard basis, $(|00\rangle, |01\rangle, |10\rangle, |11\rangle)$, the corresponding density matrix takes the form

$$\varrho^{(1)} = \begin{bmatrix} qa^2 & 0 & 0 & qa\sqrt{1-a^2} \\ 0 & (1-q)(1-a^2) & (1-q)a\sqrt{1-a^2} & 0 \\ 0 & (1-q)a\sqrt{1-a^2} & (1-q)a^2 & 0 \\ qa\sqrt{1-a^2} & 0 & 0 & q(1-a^2) \end{bmatrix}. \tag{11}$$

Let us take $a^2 > q > \frac{1}{2}$. Then the first inequality (9) is violated, while the second one (10) is not. Thus the composite system can be called “quantum” with respect to the subsystem A and “classical” with respect to the subsystem B . One may then expect that the bipartite system will lose en-

tanglement in different ways, depending on whether the environment interacts with classical or quantum subsystem. Intuitively one could guess that the entanglement should be more robust if the noise affects the classical subsystem.

Here we studied the system $\rho^{(1)}$ for $q=3/5$ and $a^2=3/4$.

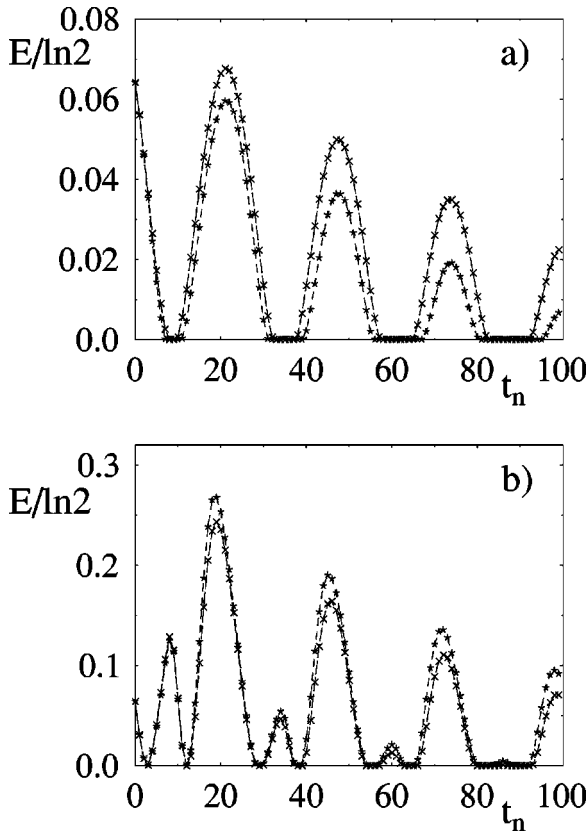


FIG. 8. Unitary dynamics and asymmetry of entanglement decay: (a) the state $\varrho^{(1)}$ defined by parameters $a^2=3/4$ and $q=3/5$ subjected to the bistochastic channel \tilde{p}_3 with $\epsilon=0.002$ and unitary dynamics H with $\alpha=0.06$ (\star); the symmetric state $\varrho^{(2)}$ interacting with the reflected Hamiltonian H' (\times). Panel (b) shows the data for reflected unitary dynamics; the Hamiltonians H' and H are exchanged.

Then von Neumann entropy of the entire system, $S=s(2/5) \approx 0.673$ is greater than the entropy of the classical subsystem B for which $S_B=s(1/4) \approx 0.562$, and smaller than the entropy of the quantum subsystem, $S_A=s(9/20) \approx 0.688$, where s stands for the binary Shannon entropy, $s(x) := -x \ln x - (1-x) \ln(1-x)$. We analyzed the time evolution of this quantum system in presence of a depolarizing channel $\Theta_{3,\epsilon}^0$ given by Eq. (2). In the theory of error-correcting codes it is one of the most popular models of environment-induced noise. The evolution of entanglement for the state $\varrho^{(1)}$ is represented by stars in Fig. 7. In this case the bistochastic channel $\tilde{\Lambda}$ acts on the “classical” subsystem B . To investigate a possible asymmetry of the entanglement decay we consider the state $\rho^{(2)}$, for which both subsystems are exchanged. More precisely, all elements of both density matrices are equal, apart from $\rho_{23}^{(2)} = \rho_{32}^{(1)}$ and $\rho_{32}^{(2)} = \rho_{23}^{(1)}$. The corresponding dynamics of $\rho^{(2)}$ is denoted by crosses in Fig. 7. In this case the noise interacts with the “quantum” subsystem A . The magnification in the inset reveals the asymmetry in the time evolution. Observe that the attack on the “classical” part of the system is more harmful to the entanglement properties of the sys-

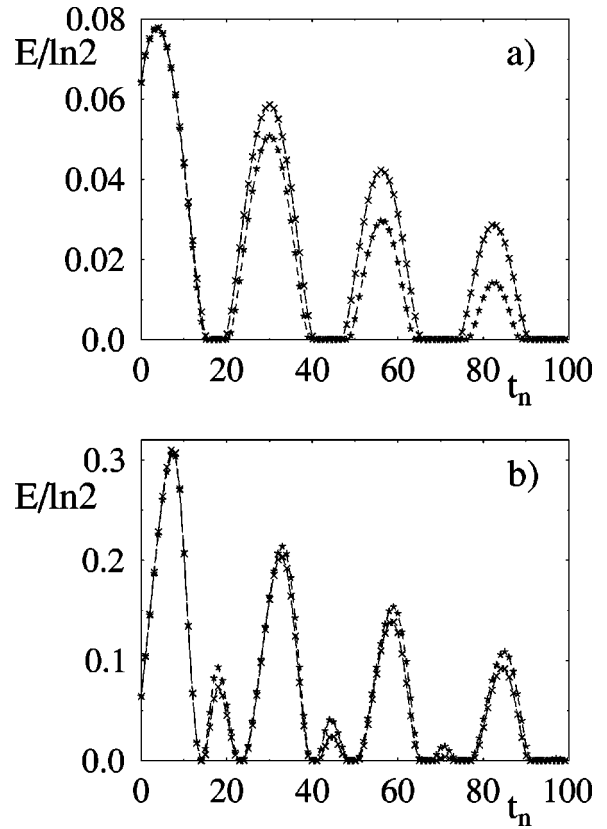


FIG. 9. As in Fig. 8 for $\epsilon=0.002$ and $\alpha=-0.06$, i.e., the process runs back in time. Observe that maxima in Fig. 8(a) correspond to minima in (a) and vice versa.

tem. This counterintuitive effect, called subsequently anomalous entanglement decay (AED), links quantum and classical features of the state from information-theoretical point of view.

Let us recall that any $2 \otimes 2$ system may be described by two Bloch vectors, representing locally both subsystems, and a correlation matrix T , which represents the projection of the composite system onto the family of mixtures of maximally entangled states (see [20]). A possible explanation of AED should take into account the fact that the local action of environment changes both the Bloch vectors, the correlation matrix, as well as their relationship. A depolarizing channel may affect in a similar way both local parameters, but it may distinguish, in sense of the destruction of the entanglement, the correlation parameters with respect to the side of the action.

It should be noted that, regardless of which part is subjected to the noise, the entanglement of mixed states $\rho^{(1)}$ and $\rho^{(2)}$ decreases slower than the entanglement of the maximally entangled states (bold line in Fig. 7). This is due to the fact that the latter decreases fast for short times and slow at longer time scales, for which the initially pure state gets mixed. It is thus instructive to compare the shape of the bold line starting from $t_N \approx 60$ with the symbols representing the initial decay of entanglement of the states $\rho^{(i)}$.

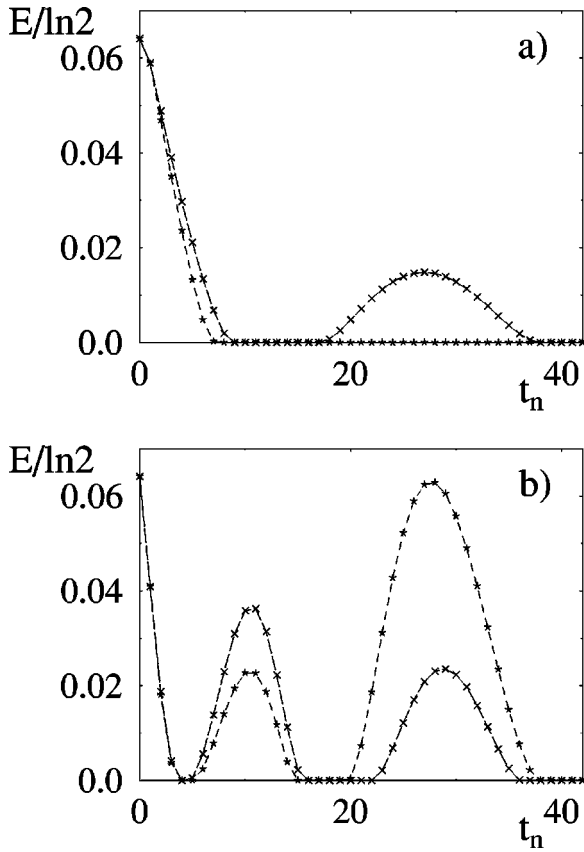


FIG. 10. As in Fig. 8 for $\epsilon=0.01$ and $\alpha=0.04$.

VI. AMPLIFYING THE PROCESSES: ENTANGLEMENT REVIVALS

Consider now the depolarizing dynamics $\Theta_{\alpha,\epsilon}^3$ with an unitary operation involved, ($\alpha \neq 0$), affecting either subsystem *A* or *B*. To compare the dynamics of both symmetric mixed states $\rho^{(1)}$ and $\rho^{(2)}$ we study their unitary interaction governed by the Hamiltonians: $H = \sigma_x \otimes \sigma_y$, and the reflected one $H' = \sigma_y \otimes \sigma_x$.

Let us consider two cases:

- (a) the noise parameter ϵ is much less than the parameter α characterizing the unitary interaction,
- (b) both parameters are of the same order of magnitude.

Numerical results obtained in the weak noise case (a) are presented in Figs. 8 and 9. The revivals of the entanglement, caused by the unitary interaction, are manifestly visible, since the strength of the interaction with the environment $\epsilon = 0.002$ is much less than the parameter $\alpha = 0.06$ governing the unitary dynamics. Note the characteristic entanglement plateaus, if the analyzed state travels across the set of the separable states and the entanglement attains its minimal value equal to zero. The effect of anomalous entanglement decay is clearly visible in Fig. 8(a), where the entanglement decays faster if the environment interacts with the classical subsystem. This contrasts the situation shown in Fig. 8(b), for which the unitary evolution is due to the reflected Hamiltonian H' and the exposure of the quantum subsystem to the

action of the environment action is more damaging for the entanglement.

It is instructive to analyze the same system with the unitary evolution reversed in time. Such a case, obtained by a change of the parameter $\alpha \rightarrow -\alpha$, is presented in Fig. 9. The general character of the evolution is kept. The significant difference is that here the entanglement is *amplified* at the very beginning that may have practical consequences if we are interested in short times of the process. Note that Figs. 8(a) and 9(a) reflected along the vertical line at $t_n=0$ [respectively, 8(b) and reflected 9(b)] exhibit some kind of symmetry with respect to the initial moment.

What happens if we allow the strength of the coupling with the environment to be comparable with the parameter of the unitary interaction? This situation, corresponding to the case (b), is illustrated in Fig. 10. Here some interesting qualitative changes occur. The AED effect is present in the case shown in Fig. 10(a), at the beginning the entanglement disappears faster when the classical part of the system is affected by the environment. Moreover, in this case the entanglement disappears completely and never revives. If the quantum subsystem interacts with the environment, a single *entanglement revival* occurs.

In the complementary case, for which $\rho^{(1)}$ interacts with the reflected Hamiltonian H' [see 10(b)], we observe a special kind of competition: for short times the entanglement is smaller, if the quantum subsystem is perturbed. For longer times, the roles are interchanged, and the oscillations of the entanglement are damped faster, if the classical subsystem interacts with the environment.

In general one can see that the pictures corresponding to the cases (a) and (b) are qualitatively different depending on the ratio ϵ/α . This fact may be related to the observation concerning the processes of decoherence. Depending on the relation between two coupling parameters the so called *pointer basis* is determined either by the internal self-Hamiltonian of the system or by the Hamiltonian of the interaction with environment [3].

VII. DISCUSSION

We investigated the behavior of entanglement of bipartite spin-1/2 system subjected to periodic action of the environment. The process of destruction of entanglement of initially pure states is accompanied by increasing of von Neumann entropy. The asymptotic value of the entropy depends on the form of the interaction with the environment. For strongly mixing bistochastic channels, e.g., Θ^2 and Θ^3 , the entropy achieves the maximal value $\ln 4$. If the decaying channel is involved, the entropy gets its maximum and then it monotonically decays to the asymptotic value, which reveals the initial entanglement of the system.

If the internal unitary evolution entangling the system is present, the decay of the entropy due to the decaying channel can be replaced by the process of mixing the state more and more. The general feature of the time evolution is that the entanglement decreases as the system becomes more mixed. This corresponds to the results recently presented in Refs. [14,15], where it was shown that the mean entanglement of

quantum states, averaged over a sample of mixed states with the same von Neumann entropy, decreases with the degree of mixing. The presence of the internal unitary evolution leads to the revivals of the entanglement and to suppression (or acceleration) of the entanglement decay.

Perhaps the most intriguing is the character of asymmetry of the time evolution of the entanglement. For some initial mixed states consisting of two nonequivalent subsystems, the entanglement decays faster, if the environment interacts with the classical subsystem, which satisfies the entropic inequality. Many years ago Schrödinger considered entanglement of pure state as a property of having both subsystems less informative for the observer, than the composite system. Mixed states (11) considered here exhibit this property only with respect to one subsystem [19]. Our results show that the action of environment to the classical subsystem is sometimes more harmful to the entanglement. In this case one can thus say that the *quantum entanglement runs away faster through the classical door*.

In the context of the above discussion some general questions emerge. Consider a quantum entangled state ρ with, say, $S(\rho_A) > S(\rho_B)$, not necessarily violating the inequality (9). Under which conditions the entanglement is less robust to action of the environment on this subsystem, for which the entropy of the reduced operator is smaller? How is it related to a possible violation of the von Neumann entropy inequality by subsystem A? What happens if instead of the inequalities (9) and (10) one applies the generalized α -entropies inequalities [18,19,21] satisfied for classical systems? All these questions seem to be important for a deeper understanding of the dynamics of quantum entanglement.

It would be also interesting to analyze the role of entropic asymmetric states like Eq. (11) in context of quantum communication. In fact these states have only one coherent information positive [22,23] (see also [24]). For the corresponding quantum channels this might imply an asymmetry in the transfer of quantum information with respect to its direction, ($A \rightarrow B$ or $B \rightarrow A$).

Finally, the obtained results show that even the simplest bipartite systems may exhibit nontrivial properties from the point of view of the information theory. In this context it would be important to investigate further the dynamics of mixed entanglement, in particular, by taking into account the phenomenon of bound entanglement [25].

ACKNOWLEDGMENTS

It is a pleasure to thank the European Science Foundation and the Newton Institute for a support during our stay in Cambridge, where this work has been initiated. K.Ż. is supported by Polish Committee for Scientific Research, Contract No. 2 PO3B 072 19. M. P. R. H. are supported by Polish Committee for Scientific Research, Contract No. 2 P03B 103 16 and by European Community under the IST project EQUIP, Contract No. IST-1999-11053.

APPENDIX: RANDOM PURE STATES

In this appendix we present algorithms allowing one to generate random quantum states distributed uniformly in the entire space of pure states, the manifold of separable pure states and the space of maximally entangled pure states. We concentrate here on the simplest $2 \otimes 2$ problem, but the algorithms below can be easily generalized for higher dimensions.

1. Generation of random pure states

The set of pure states of a four-dimensional (4D) Hilbert space forms a complex projective space CP^3 , on which a natural, unitarily invariant measure exists. To generate random pure states according to such a measure on this six-dimensional space we take a vector of a random unitary matrix distributed according to the Haar measure on $U(4)$. The Hurwitz parametrization [26] gives

$$|\Psi\rangle = (\cos \vartheta_3, \sin \vartheta_3 \cos \vartheta_2 e^{i\varphi_3}, \sin \vartheta_3 \sin \vartheta_2 \cos \vartheta_1 e^{i\varphi_2}, \sin \vartheta_3 \sin \vartheta_2 \sin \vartheta_1 e^{i\varphi_1}), \tag{A1}$$

where $\vartheta_k \in [0, \pi/2]$, and $\varphi_k \in [0, 2\pi)$ for $k=1,2,3$.

A uniform distribution over almost all of CP^3 is obtained by choosing the uniform distribution of the ‘‘azimuthal’’ angles; $P(\varphi_k) = 1/2\pi$. In the analogy to the volume element on the sphere the ‘‘polar’’ angles ϑ_k should be taken in a nonuniform way, with the probability density [26]

$$P(\vartheta_k) = k \sin(2\vartheta_k) (\sin \vartheta_k)^{2k-2} \tag{A2}$$

for $\vartheta_k \in [0, \pi/2], k=1,2,3$. In practice it is convenient to use auxiliary independent random variables ξ_k distributed uni-

formly in $[0, 1]$ and to set $\vartheta_k = \arcsin(\xi_k^{1/2k})$. The above formula with $k=1,2,\dots,N-1$ allows one to get a natural distribution on CP^{N-1} [27].

2. Random separable pure states

Any $2 \otimes 2$ pure separable state may be written as $|\Psi_s\rangle = |\psi_1\rangle \otimes |\psi_2\rangle$, where $|\psi_1\rangle$ and $|\psi_2\rangle$ are $N=2$, one-particle pure states. The four-dimensional manifold of separable states has thus a simple structure of a Cartesian product $CP^1 \times CP^1$. A uniform measure on this manifold is obtained by taking both states $|\psi_i\rangle$ distributed uniformly (and independently) at the Bloch sphere, $CP^1 \sim S^2$.

Working in the standard basis,

$$|\Psi_s\rangle = U_1 \otimes U_2 |(1,0,0,0)\rangle, \quad (\text{A3})$$

where U_1 and U_2 denote two independent random unitary matrices distributed uniformly on $SU(2)$. This parametrization describes the entire 4D manifold of the separable pure states.

3. Random maximally entangled states

In an analogous way we may represent the maximally entangled states as

$$|\Psi_e\rangle = \mathbb{1} \otimes U_1 |(0,1,1,0)/\sqrt{2}\rangle. \quad (\text{A4})$$

It is easy to see that for these states the reduced density matrix is proportional to identity matrix, and the entropy of entanglement achieves its maximum, $\ln 2$. The states ob-

tained by a symmetric operations $U_1 \otimes \mathbb{1}$ are also maximally entangled. Using the standard representation of U_1 we parametrize maximally entangled states by [28]

$$|\Psi_{e1}\rangle = \frac{1}{\sqrt{2}} \begin{bmatrix} \cos \vartheta e^{i\varphi_1} \\ \sin \vartheta e^{i\varphi_2} \\ -\sin \vartheta e^{-i\varphi_2} \\ \cos \vartheta e^{-i\varphi_1} \end{bmatrix}. \quad (\text{A5})$$

The angles φ_i are distributed uniformly in $[0, 2\pi)$, whereas according to (A1) $P(\vartheta) = \sin(2\vartheta)$ for $\vartheta \in [0, \pi/2]$. Note that the standard element of the volume on the two spheres $dS = \sin \theta d\theta d\varphi$ is written in a rescaled variable $\theta = 2\vartheta$. Given maximally entangled state corresponds to a single unitary matrix U_1 pertaining to $SU(2)$, but the 3D manifold of the maximally entangled states has the topology of the real projective space, $\mathbb{R}P^3 \sim U(3)/U(1)$ [29].

-
- [1] A. Einstein, B. Podolsky, and N. Rosen, *Phys. Rev.* **47**, 777 (1935).
- [2] E. Schrödinger, *Proc. Cambridge Philos. Soc.* **31**, 555 (1935).
- [3] W. H. Zurek, *Philos. Trans. R. Soc. London, Ser. A* **356**, 1793 (1998).
- [4] X. X. Yi and C. P. Sun, *Phys. Lett. A* **262**, 282 (1999).
- [5] K. Krauss, *Ann. Phys. (N.Y.)* **64**, 311 (1971); E. B. Davies, *Quantum Theory of Open Systems* (Academic, London, 1976).
- [6] R. Alicki and K. Lendi, *Quantum Dynamical Semigroups and Applications* (Springer-Verlag, Amsterdam, 1987).
- [7] A. Loziński and K. Życzkowski (unpublished).
- [8] P. Badziąg, M. Horodecki, P. Horodecki, P. Horodecki, and R. Horodecki, *Phys. Rev. A* **62**, 012311 (2000).
- [9] See J. Preskill, at www.theory.caltech.edu/people/preskill/ph229.
- [10] R. Penrose, *The Emperor's New Mind* (Oxford University Press, Oxford, 1989).
- [11] C. H. Bennett, D. P. DiVincenzo, J. Smolin, and W. K. Wootters, *Phys. Rev. A* **54**, 3824 (1997).
- [12] R. Horodecki and P. Horodecki, *Phys. Lett. A* **194**, 147 (1994).
- [13] S. Hill and W. K. Wootters, *Phys. Rev. Lett.* **78**, 5022 (1997); W. K. Wootters, *ibid.* **80**, 2245 (1998).
- [14] K. Życzkowski, P. Horodecki, A. Sanpera, and M. Lewenstein, *Phys. Rev. A* **58**, 883 (1998).
- [15] K. Życzkowski, *Phys. Rev. A* **60**, 3496 (1999).
- [16] S. L. Braunstein, *Phys. Lett. A* **219**, 169 (1996).
- [17] M. J. W. Hall, *Phys. Lett. A* **242**, 123 (1998).
- [18] R. Horodecki, P. Horodecki, and M. Horodecki, *Phys. Lett. A* **210**, 377 (1996).
- [19] R. Horodecki, *Phys. Lett. A* **210**, 223 (1996).
- [20] R. Horodecki and M. Horodecki, *Phys. Rev. A* **54**, 1838 (1996).
- [21] P. Horodecki, J. A. Smolin, B. M. Terhal, and A. V. Thapliyal, e-print quant-ph/9910122.
- [22] B. Schumacher, *Phys. Rev. A* **54**, 2614 (1996); B. Schumacher and M. A. Nielsen, *ibid.* **54**, 2629 (1996).
- [23] S. Lloyd, *Phys. Rev. A* **55**, 1613 (1997).
- [24] M. Horodecki, P. Horodecki, and R. Horodecki, *Phys. Rev. Lett.* **85**, 433 (2000).
- [25] M. Horodecki, P. Horodecki, and R. Horodecki, *Phys. Rev. Lett.* **80**, 5239 (1998); P. Horodecki, M. Horodecki, and R. Horodecki, *ibid.* **82**, 1056 (1999).
- [26] A. Hurwitz, *Nachr. Ges. Wiss. Goettingen, Math.-Phys. Kl.* **71**, 309 (1898); see also *Mathematische Werke von Adolf Hurwitz, Band II* (Birkhauser, Basel, 1933), p. 563.
- [27] M. Poźniak, K. Życzkowski, and M. Kuś, *J. Phys. A* **31**, 1059 (1998).
- [28] M. Kuś and K. Życzkowski, *Phys. Rev. A* **63**, 032307 (2001), LANL e-print quant-ph/0006068.
- [29] K. G. H. Vollbrecht and R. F. Werner, *J. Math. Phys.* **41**, 6772 (2000).